**Author(s)** Müller, Juliane; Piché Robert

**Title** Mixture surrogate models based on Dempster-Shafer theory for global optimization problems

**Citation** Müller, Juliane; Piché, Robert 2011. Mixture surrogate models based on Dempster-Shafer theory for global optimization problems. Journal of Global Optimization vol. 51, num. 1, 79-104.

**Year** 2011

**DOI** http://dx.doi.org/10.1007/s10898-010-9620-y

**Version** Post-print

**URN** http://URN.fi/URN:NBN:fi:tty-201311011411

**Copyright** The final publication is available at link.springer.com.

# Mixture Surrogate Models Based on Dempster-Shafer Theory for Global Optimization Problems

**Juliane Müller · Robert Piché**

**Abstract** Recent research in algorithms for solving global optimization problems using response surface methodology has shown that it is in general not possible to use one surrogate model for solving different kinds of problems. In this paper the approach of applying Dempster-Shafer theory to surrogate model selection and their combination is described. Various conflict redistribution rules have been examined with respect to their influence on the results. Furthermore, the implications of the surrogate model type, i.e. using combined, single or a hybrid of both, have been studied. The suggested algorithms were applied to several well-known global optimization test problems. The results indicate that the used approach leads for all problems to a thorough exploration of the variable domain, i.e. the vicinities of global optima could be detected, and that the global minima could in most cases be approximated with high accuracy.

**Keywords** Global optimization, Mixture surrogate models, Dempster-Shafer theory, Response surface

## 1 Introduction

The development and optimization of new products and engineering designs requires computationally expensive simulations due to the complexity of the underlying processes. In order to obtain the response of the system at one point it might be necessary to solve large systems of differential equations or to do some other time consuming numerical simulations. Thus, using these simulation models during the optimization process will lead to prohibitively high computation times as commonly used optimization routines require many function evaluations. Furthermore, these optimization routines usually converge to a local optimum close to the chosen starting point.

Surrogate models have been developed in order to reduce the necessary number of costly simulations while searching for the global optimum of the problem at hand. The advantage of surrogate models is their low computational complexity compared to the true simulation model. In general, a surrogate model can be represented by

$$f(\mathbf{x}) = s(\mathbf{x}) + \epsilon,$$

where $f(\mathbf{x})$ denotes the output of the simulation model (also referred to as true model) at the point $\mathbf{x}$, $s(\mathbf{x})$ denotes the output of the surrogate model, and $\epsilon$ represents the error between both.

Surrogate models can be either non-interpolating or interpolating [11]. Non-interpolating models include for example polynomial regression models [20] and multivariate adaptive regression splines [6]. Radial basis functions [2, 9, 22, 24, 25] and Kriging [12, 13, 17, 18] are interpolating surrogate models.

J. Müller
Tampere University of Technology, Department of Mathematics
P.O. Box 553, FI-33101 Tampere, Finland
E-mail: juliane.mueller@tut.fi

R. Piché
Tampere University of Technology, Department of Mathematics
P.O. Box 553, FI-33101 Tampere, Finland
E-mail: robert.piche@tut.fi

Surrogate models have for example been used by [7] during the optimization of helicopter rotor blades, or also by [23] who designed a liquid-rocket injector with respect to multiple objectives. Efficient Global Optimization (EGO) has been applied by [19] in order to optimize the shape of horn-loaded loudspeakers. Surrogate models have also been used in automotive design (see for example [14, 30, 32]).

However, as shown for example by [8] and [28], one surrogate model does not suit all kinds of problems, i.e. a certain surrogate model might perform very well on some problem type, but badly for other problems. If it is not known beforehand which surrogate model is the most suitable for the problem at hand, different models or also mixture models have to be tried in order to find the most effective one. Then, the challenge is the determination of the best surrogate model and the adjustment of the influence of single surrogate models in mixtures, respectively. The prediction $\hat{y}(\mathbf{x})$ of such a mixture surrogate model can in general be represented as

$$\hat{y}(\mathbf{x}) = \sum_{i=1}^{N} w_i \hat{y}_i(\mathbf{x}), \ \sum_{i=1}^{N} w_i = 1, \tag{1}$$

where $\hat{y}_i(\mathbf{x})$ denotes the prediction of the $i$th contributing model, $w_i \geq 0$ is the corresponding weight, and $N$ is the number of models.

Goel *et al.* [8] suggested different approaches for determining the weights of models in combinations. However, only one of the approaches allows emphasizing and restricting the influence of good and bad model characteristics, respectively. Moreover, in this approach parameters that are in general unknown must be adjusted beforehand. Viana and Haftka [28] also considered mixture surrogate models and suggested the optimization of an auxiliary function in order to obtain an approximation matrix. This matrix is in turn used for determining the model weights, but it can lead to negative weights and weights larger than one, and thus results may become inaccurate.

In order to overcome the mentioned problems the choice and combination of different surrogate models via Dempster-Shafer theory [4, 26] will be considered in this paper. Dempster-Shafer theory (DST) is a mathematical theory of evidence which provides means of combining information from different sources in order to construct a degree of belief. The theory allows the combination of imprecise and uncertain pieces of information which may even be conflicting. So-called basic probability assignments (BPA) contain information about certain hypotheses (focal elements) and are combined in order to calculate the credibility of a given hypothesis. Three functions are usually associated with BPAs, namely the belief (Bel), plausibility (Pl) and pignistic probability (BetP) function.

In terms of surrogate models the BPAs can be, for example, model characteristics such as correlation coefficients and root mean squared errors (RMSE). It is possible that one surrogate model has conflicting characteristics, i.e. good (e.g. high correlation coefficients) and bad (e.g. high RMSE) characteristics. This conflict must be considered when calculating the belief one has in the given model. Several conflict redistribution rules have been developed in the literature. Dempster's rule of combination redistributes the conflict amongst all focal elements, regardless of which elements caused the conflict. However, as shown by [31], the results of this approach may be counter-intuitive. Other ways of distributing the conflict in a fairer way have been developed: the conflict can be assigned to the set reflecting complete ignorance [29], or one may apply the proportional conflict redistribution (PCR) rules [27] to redistribute the conflict among those focal elements that cause the conflict. The disadvantage of the latter approach is however the computational complexity which increases with the number of information sources. Inagaki [10] proposes a general formulation for the redistribution of the conflict incorporating parameters which in turn may influence the result of the information combination.

The goal of this paper is to apply Dempster-Shafer theory in order to choose amongst different surrogate models the most suitable one for a given optimization problem, and to find the weights of single models contributing to combinations, respectively. It is necessary to guarantee a thorough global and local exploration of the variable domain. Regions where the global optimum may be located must be examined thoroughly, but the algorithm must also not get stuck in a local optimum. Since it is in general unknown whether mixture models will be more successful than single models, the following alternative strategies shall be examined:

1. using the best mixture model for the first optimization steps, then switching to using always the best single surrogate model,
2. using only the best mixture model,
3. using only the best single surrogate model.

The remainder of this paper is organized as follows. The considered surrogate models are briefly described in Section 2. A description of the algorithm is given in Section 3, and the results for different test problems are given in Section 4. Section 5 concludes the paper and future research topics are outlined.

## 2 Surrogate Models

In the following it is assumed that the true function $f : \mathbb{R}^k \mapsto \mathbb{R}$ has been sampled at $n$ points of the domain according to some given experimental design. Denote those sample sites by $\mathbf{x}_1, \mathbf{x}_2, \ldots, \mathbf{x}_n$, $\mathbf{x}_i \in \mathbb{R}^k\ \forall i$, and the corresponding function values by $y_1, y_2, \ldots, y_n$. Based on the given experimental design surrogate models are built. The considered model types will be described next.

Polynomial regression models of different degrees can be easily built using the method of least squares. In general, models of degree two are in most cases sufficient. The inclusion of cross terms is in many application problems important since they reflect the interaction between different variables. Thus, considered are polynomial regression models of second order which can be represented by

$$y_i(\mathbf{x}_i) = \beta_0 + \sum_{j=1}^{k} \beta_j x_{ij} + \sum_{j=1}^{k} \beta_{jj} x_{ij}^2 + \sum_{j_1=1}^{k} \sum_{\substack{j_2=1 \\ j_2 \neq j_1}}^{k} \beta_{j_1 j_2} x_{i,j_1} x_{i,j_2} + \epsilon_i, \quad i = 1, 2, \ldots, n,$$

where $\beta_i$, $i = 0, \ldots, n$, are parameters to be determined.

Multivariate adaptive regression splines (MARS) is a non-parametric regression technique introduced by [6]. The method can be interpreted as an extension of linear models to include non-linearities and interactions. In general MARS models are of the form

$$\hat{y}(\mathbf{x}) = \sum_{i=1}^{m} a_i B_i(\mathbf{x}),$$

where $a_i$ are constant coefficients, and $B_i(\mathbf{x})$ are basis functions. Basis functions can either be just a constant, i.e. the intercept, a hinge function of the form $\max\{0, x - \text{const}\}$ or $\max\{0, \text{const} - x\}$, or the product of two or more hinge functions representing interactions between variables. The MARS model is built in two phases, namely a forward and backward iterative approach, where the basis functions are adaptively selected in order to approximate the true function.

Radial basis functions have been introduced by [5] and with their help the curvature of the true function can be modeled well. The surrogate model is defined by

$$\hat{y}(\mathbf{x}) = \sum_{i=1}^{n} \lambda_i \phi\left(\|\mathbf{x} - \mathbf{x}_i\|_2\right) + p(\mathbf{x}), \tag{2}$$

where $\|\cdot\|$ denotes the Euclidean norm, $\lambda_1, \lambda_2, \ldots, \lambda_n \in \mathbb{R}$, $\phi : \mathbb{R}_+ \mapsto \mathbb{R}$ are radial basis functions, and $p(\mathbf{x})$ denotes an optional polynomial tail of the form $\mathbf{b}'\mathbf{x} + a$, $\mathbf{b} \in \mathbb{R}^k, a \in \mathbb{R}$. Frequently used radial basis functions are, for example, cubic, thin plate spline, Gaussian, multiquadric, and inverse-multiquadric. The required parameters are determined by solving the linear system

$$\begin{bmatrix} \boldsymbol{\Phi} & \mathbf{P} \\ \mathbf{P}' & \mathbf{0} \end{bmatrix} \begin{bmatrix} \boldsymbol{\lambda} \\ \mathbf{c} \end{bmatrix} = \begin{bmatrix} \mathbf{F} \\ \mathbf{0} \end{bmatrix}, \text{ where } \mathbf{P} = \begin{bmatrix} \mathbf{x}_1' & 1 \\ \mathbf{x}_2' & 1 \\ \vdots & \vdots \\ \mathbf{x}_n' & 1 \end{bmatrix}, \quad \boldsymbol{\lambda} = \begin{bmatrix} \lambda_1 \\ \lambda_2 \\ \vdots \\ \lambda_n \end{bmatrix} \quad \mathbf{c} = \begin{bmatrix} b_1 \\ b_2 \\ \vdots \\ b_k \\ a \end{bmatrix}, \quad \mathbf{F} = \begin{bmatrix} y_1 \\ y_2 \\ \vdots \\ y_n \end{bmatrix},$$

and $\boldsymbol{\Phi}$ is an $n \times n$ matrix with entries $\Phi_{ij} = \phi\left(\|\mathbf{x}_i - \mathbf{x}_j\|_2\right)$. Then, if rank($P$)= k+1, the matrix $\begin{bmatrix} \boldsymbol{\Phi} & \mathbf{P} \\ \mathbf{P}' & \mathbf{0} \end{bmatrix}$ is nonsingular and the linear system has a unique solution [21]. Therefore, it is possible to obtain a unique radial basis function interpolant to the true function $f$.

Kriging was developed by the French mathematician Georges Matheron [18] and was first used in numerical experiments in 1988 [3]. Kriging models consist of two components. The first component is some simple model which captures the trend in the data, whereas the second component is stochastic and measures the deviation between the simple model and the true function. A model $\hat{y}$ is built as a realization of a regression model and a random function $z$ in order to express the deterministic response $y$ for the input:

$$\hat{y}(\mathbf{x}) = \sum_{j=1}^{p} \beta_j \phi(\mathbf{x}) + z(\mathbf{x}),$$

where the regression model basis functions $\phi_j : \mathbb{R}^k \mapsto \mathbb{R}$, and $\beta_1, \dots, \beta_p$ are the regression coefficients. The random process $z$ is assumed to have zero mean and covariance depending on an underlying correlation model, including parameters that must be optimized. Commonly used correlation functions are, for example, exponential, generalized exponential, Gaussian, spherical, or spline, whereas regression models can be chosen, for example, to be constant, linear or quadratic [15].

## 3 Mixture Surrogate Model Algorithm

This section details the algorithm for solving global optimization problems. The algorithm starts by generating an experimental design using Latin hypercube sampling (LHS) which maximizes the minimum distance between the design points. The minimal number of initial sample sites is problem dependent. In general, at least $n + 1$ initial design sites are required for building the models. However, since in a later stage leave-one-out cross validation is used to assess the accuracy of the models, at least one additional initial sample site must be taken. Thus, if for example a two dimensional problem is considered, one needs at least four sample sites in the initial experimental design.

Given the $n + 2$ sample sites and the corresponding expensive function values, the leave-one-out cross validation is applied, as follows. One sample site is left out from the experimental design, and the remaining sample sites and their corresponding function values are used to build the surrogate model, which is then used to predict the value at the sample site that was left out. This is done for every surrogate model type and every sample site, and thus for every sample site a prediction from every model is obtained.

Correlation coefficients (CC), root mean squared errors (RMSE), maximal absolute errors (MAE) and median absolute deviation (MAD) have been chosen as model characteristics. They are calculated for every model based on the true and the predicted responses. Characteristics of a good model are high positive correlation coefficients, low RMSE, as well as low MAE and low MAD. The number and type of model characteristics should in general be tailored to specific application problems, but this paper is restricted to the aforementioned numerical values.

After the model characteristics have been calculated BPAs are computed for every model. For this purpose the model characteristics are scaled so that the sum over all models for each BPA equals one and the non-negativity conditions of BPAs are fulfilled. Dempster-Shafer theory is applied in order to find the pignistic probabilities for each model. Based on these values it can be decided which of all considered models is the best, or in case mixture models are considered, which weight should be assigned to each contributing model.

When considering mixture models CC, RMSE, MAE and MAD must also be calculated for each mixture in order to find the best one. The goodness values are normalized to obtain the BPAs for each mixture:

$$m_i^{\text{CC}} = \frac{\text{CC}_i}{\sum_{j\in\mathcal{M}} \text{CC}_j},\ m_i^{\text{RMSE}} = \frac{\frac{1}{\text{RMSE}_i}}{\sum_{j\in\mathcal{M}} \frac{1}{\text{RMSE}_j}},\ m_i^{\text{MAE}} = \frac{\frac{1}{\text{MAE}_i}}{\sum_{j\in\mathcal{M}} \frac{1}{\text{MAE}_j}},\ m_i^{\text{MAD}} = \frac{\frac{1}{\text{MAD}_i}}{\sum_{j\in\mathcal{M}} \frac{1}{\text{MAD}_j}},$$

where $\mathcal{M}$ is the set of models contributing to the combination. Thus, four evidence sets are obtained. In other words, the models contained in each considered mixture build the focal elements and the evidence sets are the BPAs which will in turn be used in the decision theory.

In order to illustrate the above procedure consider the following example. Assume the four models described in Section 2 are available and denote the polynomial model by P, the RBF model by R, the Kriging model by K, and the MARS model by M. After cross-validation the characteristics of the single models are as follows:

$$\begin{array}{llll} m_{\mathrm{P}}^{CC} = 0.29, & m_{\mathrm{R}}^{CC} = 0.29, & m_{\mathrm{K}}^{CC} = 0.42, & m_{\mathrm{M}}^{CC} = 0 \\ m_{\mathrm{P}}^{RMSE} = 0.11, & m_{\mathrm{R}}^{RMSE} = 0.24, & m_{\mathrm{K}}^{RMSE} = 0.25, & m_{\mathrm{M}}^{RMSE} = 0.40, \\ m_{\mathrm{P}}^{MAE} = 0.10, & m_{\mathrm{R}}^{MAE} = 0.24, & m_{\mathrm{K}}^{MAE} = 0.25, & m_{\mathrm{M}}^{MAE} = 0.41, \\ m_{\mathrm{P}}^{MAD} = 0.17, & m_{\mathrm{R}}^{MAD} = 0.27, & m_{\mathrm{K}}^{MAD} = 0.26, & m_{\mathrm{M}}^{MAD} = 0.30. \end{array}$$

After applying DST the pignistic probabilities of the models are

$$\mathrm{BetP(P)} = 0.05,\ \mathrm{BetP(R)} = 0.40,\ \mathrm{BetP(K)} = 0.55,\ \mathrm{BetP(M)} = 0,$$

and thus, if a single model was used in the next step, the Kriging model would be chosen. If however a mixture model is required, the given pignistic probabilities are used for calculating the weights of the contributing models. Assume that models P and R are supposed to be combined. Then the weights for both models are

$$w_{\mathrm{P}} = \frac{\mathrm{BetP(P)}}{\mathrm{BetP(P)} + \mathrm{BetP(R)}},\ w_{\mathrm{R}} = \frac{\mathrm{BetP(R)}}{\mathrm{BetP(P)} + \mathrm{BetP(R)}},$$

respectively. Thus $w_{\mathrm{P}} + w_{\mathrm{R}} = 1$, and these weights are used to build the model estimate according to (1):

$$\hat{y}(\mathbf{x}) = w_{\mathrm{P}}\hat{y}_{\mathrm{P}}(\mathbf{x}) + w_{\mathrm{R}}\hat{y}_{\mathrm{R}}(\mathbf{x}),$$

where $\hat{y}_{\mathrm{P}}(\mathbf{x})$ and $\hat{y}_{\mathrm{R}}(\mathbf{x})$ are the predictions of the polynomial and RBF model at the point $\mathbf{x}$, respectively.

The algorithm considers every possible (one-,) two-, three- and four-model mixture, and therefore the focal elements to be considered are {P}, {R}, {K}, and {M} for the single models, {P,R}, {P,K}, {P,M}, {R,K}, {R,M}, and {K,M} for the two-model combinations, {P,R,K}, {P,R,M},{P,K,M}, and {R,K,M} for the three-model combinations, and {P,R,K,M} for the four-model combination. In case of mixture models BPAs must be calculated based on the cross validation characteristics of the corresponding mixture.

In the next step, one of the described conflict redistribution rules from Section 1 is applied, i.e. the evidences obtained are combined, and for each mixture and single model the corresponding belief, plausibility and pignistic probability is calculated. Then the (mixture) model with the highest plausibility value is chosen as new response surface[1].

Next a new sample site must be chosen. The algorithm must guarantee a thorough local as well as a global search, i.e. the algorithm should be able to find objective function valleys and sample there several times, but must also be prevented from getting stuck in a local optimum. The difficulty is to decide when to interrupt the local search, i.e. after how many samples in a certain region the search should continue in a more global manner and vice versa.

If sites of the minima of the single models contributing to the mixture model are very distant from each other, it might be an indication that there are several regions in the variable domain where local or global optima could be located, and thus sampling at these points may be favorable. However, if the sites are close together, this approach may lead to a very local search.

In order to prevent the algorithm from excessive sampling in the vicinity of the currently best point it is necessary to force the search away from regions where already many samples have been taken. For this purpose the minimal distances $d_{\min}$ between every newly added sample site and all other already sampled points are recorded, and in case a certain amount of sample sites closer to each other than some predefined threshold distance $d^*$ is exceeded, the algorithm must be prevented from adding more points in the already densely sampled region. The smaller the number of allowed close points is, the more global the search becomes. On the other hand, increasing the maximal allowed number of close samples leads to a longer local search which adds more sample points in the vicinity of the currently best known point. Similarly, the smaller the threshold distance $d^*$, the more thorough the local search becomes.

[1] Note that the combination of all models, i.e. the universal set, always has plausibility and belief values of one, and must thus be considered separately.

The sample sites where the true function has already been evaluated are clustered according to a $k$-means algorithm [16], where the number of clusters $k$ is determined dynamically. If a large cluster has been found, a densely-sampled area is defined based on the cluster's content. Denote $\mathbf{X}_{c_k} = \left[\mathbf{x}_{c_k,1}, \mathbf{x}_{c_k,2}, \ldots, \mathbf{x}_{c_k,k}\right]'$ the matrix of sample sites contained in the considered cluster $c_k$, where $\mathbf{x}_{c_k,i}$ are column vectors. Lower bounds $[\min \mathbf{X}_{c_k}(:, i_1), \ldots, \min \mathbf{X}_{c_k}(:, i_k)]$ and upper bounds $[\max \mathbf{X}_{c_k}(:, i_1), \ldots, \max \mathbf{X}_{c_k}(:, i_k)]$ are defined for the variables $i_1, \ldots, i_k \in \{1, 2, \ldots, k\}$ that are closest to each other, and thus determine the boundary of the densely-sampled area. Note that these bounds do not exist for all variables. This issue is important especially when problems with very long and steep valleys are considered. In such cases it is of advantage to not define bounds on all variables.

When searching for new prospective regions that may contain local or global optima a target value strategy similar to the one proposed by Jones [11] is applied. A vector $\mathbf{T} = s_{\min} - \boldsymbol{\alpha}\,(f_{\max} - f_{\min})$ represents desired function values, where $\boldsymbol{\alpha}$ is a vector of non-negative scalars (see also [9]). $s_{\min}$ stands for the minimum of the response surface, and $f_{\min}$ and $f_{\max}$ denote, respectively, the minimal and maximal function value obtained so far.

An optimization routine is applied in order to minimize an auxiliary function that represents the difference between the target values $T_i$ and the prediction of the response surface. In order to search more globally a penalty term is used to prevent the search from entering the densely-sampled area. Similarly, in the local search a penalty term is used to prevent the search from leaving the densely-sampled area. In this way the search can be drawn away from or restricted to the already thoroughly examined area.

For each target the point where the minimum has been located is recorded. These points are clustered into $\tilde{k}$ groups where $\tilde{k}$ can be varied in order to increase or decrease the amount of desired new sample sites. From each of the $\tilde{k}$ groups only the representative that reached the lowest value while optimizing the auxiliary function is chosen as new sample site. Problems arise however if the global optimum is inside (global search) or outside (local search) the densely-sampled region. This problem is addressed by setting the penalty of a point that reaches during the optimization of the auxiliary function a much better function value than any other candidate to zero.

The calculation of the minimum of the response surface and of the auxiliary function require themselves optimization routines. Two different approaches have been compared, namely a Hooke-Jeeves pattern search method and the accelerated random search algorithm described by Appel *et al.* [1]. Simulations showed that while both optimization routines led to approximately the same sample sites especially when the number of sample points was rather low, the ARS algorithm found much better solutions than the pattern search when the number of sample points is larger, i.e. the pattern search tends to get stuck in local optima despite multistart approach. An advantage of the pattern search algorithm over the ARS was the lower computation time. However, since the solution quality was considered more important, the ARS approach has been used throughout the algorithm.

For the accelerated random search approach $J$ different starting solutions are randomly sampled from the parameter domain scaled to $D = [0, 1]^k$, where $k$ denotes the dimension of the problem. The optimization is executed similarly to the description by Appel *et al.* [1]. Let $\|\cdot\|$ denote the sup-norm on $D$ and denote by $B(\mathbf{x}, r) = \{\mathbf{y} \in D : \|\mathbf{x} - \mathbf{y}\| \leq r\}$ the closed ball centered at $\mathbf{x}$ with radius $r$. With the contraction factor $c > 1$ and the precision threshold $\rho > 0$ given, the following steps are executed:

**Algorithm 1** Accelerated Random Search

```
1. Set iteration counter $n = 1$, radius $r_1 = 1$ and generate random $\mathbf{x}_{1,1}, \ldots, \mathbf{x}_{1,J}$ from a uniform distribution on $D$.
2. Given $\mathbf{x}_{n,1}, \ldots, \mathbf{x}_{n,J} \in D$ and $r_{n,1}, \ldots, r_{n,J} \in (0, 1]$, generate random $\mathbf{y}_{n,1}, \ldots, \mathbf{y}_{n,J}$ from uniform distributions on $B(\mathbf{x}_{n,1}, r_{n,1}), \ldots, B(\mathbf{x}_{n,J}, r_{n,J})$.
3. For all $i = 1, \ldots, J$:
       If $f(\mathbf{y}_{n,i}) < f(\mathbf{x}_{n,i})$, let $\mathbf{x}_{n+1,i} = \mathbf{y}_{n,i}$ and $r_{n+1,i} = 1$.
       Otherwise, let $\mathbf{x}_{n+1,i} = \mathbf{x}_{n,i}$ and $r_{n+1,i} = r_{n,i}/c$.
       If $r_{n+1,i} < \rho$, then $r_{n+1,i} = 1$.
   Increment $n := n + 1$, and go to Step 2.
```

At the end of the predefined number of iterations the best of the $J$ results is accepted as new solution and the corresponding point is used as new sample site. The ARS approach described could be implemented in parallel so as to execute the calculations for all $J$ starting points simultaneously.

After new sample sites have been determined, the true function is evaluated and new surrogate models are built. Again cross validation is used to evaluate the goodness of the models and DST is applied to either find the best single model or the weights of the models in mixtures. The pseudocode of the numerical procedure is given below.

**Algorithm 2** Mixture Surrogate Model Algorithm

```
1. Find initial set of sample points using for example LHS design, and evaluate costly objective function at
   those points.
2. Leave-one-out cross validation: sequentially leave out one sample site and function value at a time and use
   remaining data for building different response surfaces (e.g. polynomial regression model, RBF, Kriging,
   MARS); use every response surface to re-estimate the function value at the point left out when creating
   the models.
3. Calculate goodness values: CC, MAE, RMSE and MAD between true function values and re-estimated
   values for each model.
4. (a) If using best single model: use goodness values as evidences and apply Dempster-Shafer theory to
       choose the best model.
   (b) If using mixture model: use goodness values to calculate weights associated with single models; use
       weights for combining models and obtain predictions for every sample site from each mixture model;
       calculate CC, RMSE, MAD and MAE for each mixture model, and use the scaled values as evidences;
       use Dempster-Shafer-Theory to combine the evidences of the mixture models to choose the best
       mixture model.
5. Find the new sample site(s) in one of the following ways:
   (a) Local search 1: use the minimum site of the response surface;
   (b) Local search 2: define variable domains where already many samples have been taken (i.e. densely-
       sampled areas, later on referred to as allowed area) and apply target value strategy that allows search
       only from within this region;
   (c) Global search: define variable domains where already many samples have been taken (i.e. densely-
       sampled areas, later on referred to as forbidden area) and use target value strategy that allows sampling
       only outside this region;
6. Evaluate the costly objective function at the new sample site(s).
7. Update response surfaces.
8. Go to step 2.
```

The algorithm has been implemented in the following three versions:

- Version 1: initially the best mixture surrogate model is used in every iteration; after a predefined number of failed improvement trials (i.e. new samples that did not improve the current best function value) the algorithm switches to using only the best single model in every iteration
- Version 2: only the best mixture surrogate model is used in every iteration
- Version 3: only the best single model is used in every iteration.

Initially the algorithm is set to search globally. The criterion described by Holmström [9] (later on referred to as strategy A) has been used to determine whether the surface is fluctuating wildly. If the surface is fluctuating wildly, the minimum site of the response surface is added as new sample site. Otherwise, forbidden areas are defined. Target values are calculated and the auxiliary function is minimized taking into account possible forbidden areas.

The algorithm stays in the global search phase as long as function value improvements can be found. If no improvements have been obtained, the algorithm switches to the local search phase where the search for the minimum of the auxiliary function is restricted to the allowed areas. For both search phases it holds that if no restrictions are given for densely-sampled regions, the minimum of the auxiliary function is sought in the whole variable domain. Thus, local and global search reach in this case the same results.

On the other hand simulations showed that it might also be useful to include the minimum of the response surface as new sample site even if the surface is not fluctuating wildly (later on referred to as strategy B). Therefore, also this approach is examined, and thus three algorithm versions are tested with two different criteria for adding the minimum site of the response surface.

All sample sites must have a sufficient distance to each other, thus avoiding repeated sampling at the same point. In case no such new sample site can be found, an additional point which maximizes the minimal distance to all other already sampled points is used as new sample site.

## 4 Numerical Results

This section summarizes the results of the described algorithms for commonly used global optimization test problems. All problems have analytical descriptions and the locations of the global optima are known. All three algorithm versions have been used to solve six different problems. In order to average out the dependency on the initial experimental design 20 different starting designs have been generated for each problem and the algorithms were run for every design and every problem.

In the following the name, analytical description, as well as global minima and their locations are given together with the results of the applied algorithms. The results are presented in tables consisting of three sections, i.e. one section for every algorithm version. The abbreviations in the first column of each table reflect the rule for redistributing the global conflict, i.e. D stands for Dempster's, Y for Yager's, I for Inagaki's, and P for the PCR5 rule. The additional numbers 1, 2 and 3, respectively, indicate the usage of algorithm version 1, 2 and 3. The columns labeled by min, max and mean denote the minimal, maximal and average relative error of the algorithms for all 20 test runs. The figures corresponding to each test problem illustrate the distribution of the relative errors of all 20 runs in the form of box plots. Also every table and figure consists of parts (a) and (b) which reflect the usage of Holmströms criterion (strategy A) for adding the minimum site of the response surface (tables (a)), and the usage of the second criterion (strategy B) which adds the minimum of the response surface more frequently (tables (b)).

The second and third version of the algorithm were interrupted as soon as 150 function evaluations were reached. The first version consisted of two phases: at first the model combination was applied until either the current best solution has a relative error of less than 10%, no improvement has been found within 30 consecutive function evaluations, or the true function has been evaluated more than 150 times. If either of these conditions has been fulfilled, the algorithm switches to using the best single model in every iteration until the maximal number of 150 function evaluations has been reached.

In the experiments the following issues were of interest:

1. Did the algorithms find the vicinities of the global minima? If so, did they find all global minima if more than one was present?
2. Were there significant differences in the results when different conflict redistribution rules were used? If so, was there one rule that worked best for all problems?
3. How did the choice of the algorithm version influence the results?
4. How good were the results with respect to relative errors?
5. Did the conflict redistribution rule or the choice of the algorithm version influence the computation times significantly?
6. Which models were chosen and if mixture models were used, which weights were assigned to the contributing models?

### 4.1 Test Problem B: Branin Function

This is a two variable problem with $x_1 \in [-5, 10]$ and $x_2 \in [0, 15]$. The function is defined by

$$f(x_1, x_2) = \left( x_2 - \frac{5.1x_1^2}{4\pi^2} + \frac{5x_1}{\pi} - 6 \right)^2 + 10 \left( 1 - \frac{1}{8\pi} \right) \cos(x_1) + 10.$$

The function has three global minima with the minimal value $f^* = 0.3979$ at the locations $(x_1^*, x_2^*) = (-\pi, 12.275)$, $(x_1^*, x_2^*) = (\pi, 2.275)$, and $(x_1^*, x_2^*) = (3\pi, 2.475)$. Other local optima do not exist.

The results of the algorithms for this problem are summarized in Tables 1(a) and 1(b). Every initial experimental design contained four sample points. For the Branin test function the results show that algorithm version 1 achieves the minimal relative error most frequently when comparing the values achieved by the different conflict redistribution rules. Comparing however the mean relative errors achieved by the various algorithm versions shows that versions 2 and 3 reach in most cases the lowest values.

Figures 1(a) and 1(b) illustrate the distribution of the relative errors according to conflict redistribution rule and algorithm version. It can be seen that with only a few exceptions the medians of the relative errors are smaller in Figure 1(a) than the corresponding values in Figure 1(b). The figures show that the dispersion of the errors is highest whenever algorithm version 1 was used, and that in general algorithm version 2 achieved the lowest medians for each decision rule. Thus, it can be concluded that for the Branin test-function algorithm version 2 works best, i.e. choosing in every iteration always the best mixture model.

Table 1: Branin function relative errors

(a) Strategy A

| Rule | min | max | mean |
|---|---|---|---|
| D1 | 0.0000 | 0.0844 | 0.0186 |
| Y1 | 0.0000 | 0.0982 | 0.0200 |
| I1 | 0.0000 | 0.0775 | 0.0218 |
| P1 | 0.0010 | 0.0808 | 0.0158 |
| D2 | 0.0002 | 0.0272 | 0.0044 |
| Y2 | 0.0002 | 0.0216 | 0.0051 |
| I2 | 0.0001 | 0.0616 | 0.0054 |
| P2 | 0.0000 | 0.0978 | 0.0155 |
| D3 | 0.0000 | 0.0534 | 0.0110 |
| Y3 | 0.0000 | 0.0302 | 0.0060 |
| I3 | 0.0005 | 0.0224 | 0.0073 |
| P3 | 0.0000 | 0.0482 | 0.0100 |

(b) Strategy B

| Rule | min | max | mean |
|---|---|---|---|
| D1 | 0.0000 | 0.0482 | 0.0171 |
| Y1 | 0.0000 | 0.0867 | 0.0220 |
| I1 | 0.0000 | 0.0865 | 0.0287 |
| P1 | 0.0000 | 0.0460 | 0.0130 |
| D2 | 0.0000 | 0.0618 | 0.0088 |
| Y2 | 0.0001 | 0.0511 | 0.0095 |
| I2 | 0.0000 | 0.0467 | 0.0124 |
| P2 | 0.0001 | 0.0311 | 0.0055 |
| D3 | 0.0000 | 0.0182 | 0.0066 |
| Y3 | 0.0000 | 0.0361 | 0.0095 |
| I3 | 0.0000 | 0.0981 | 0.0135 |
| P3 | 0.0000 | 0.0374 | 0.0087 |

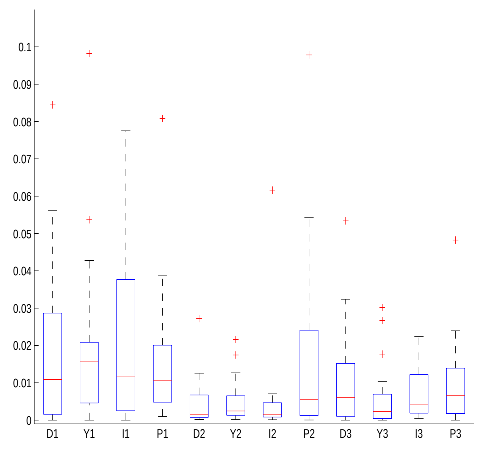

(a) Strategy A

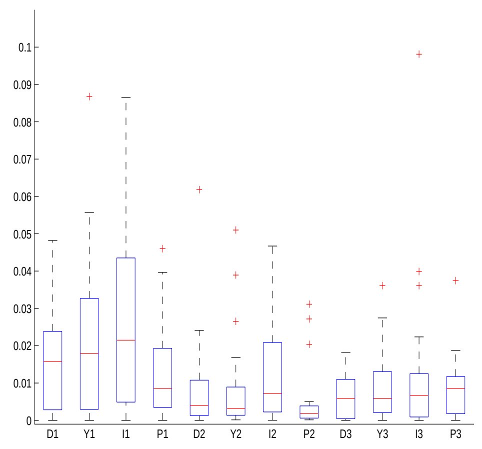

(b) Strategy B

Fig. 1: Branin function: distribution of relative errors

Examining the weights of each model when using the mixture model in algorithm version 1 shows that the Kriging model has the highest influence on the response surface. In general all four models contribute at some stage to the combination, but MARS and polynomial model have usually the lowest weights. After the switch to using in every iteration only the best single model Kriging proved best in almost all cases. For algorithm version 2 the results were similar, i.e. the Kriging model obtained the highest weights, while RBF, polynomial and MARS model contributed the least (polynomial and RBF had in general about the same weights, while the MARS model had no major impact). When choosing in every iteration only the best single model, i.e. version 3 of the algorithm, the Kriging model proved best in over 80% of all choices. MARS and the polynomial model were rarely chosen, and the RBF model was best in about 10% of all cases.

## 4.2 Test Problem C: Camelback Function

The variables of this bivariate function are constrained to $x_1 \in [-3, 3]$ and $x_2 \in [-2, 2]$ and the function is defined by

$$f(x_1, x_2) = \left(4 - 2.1x_1^2 + \frac{x_1^4}{3}\right) x_1^2 + x_1 x_2 + (-4 + 4x_2^2)x_2^2.$$

The function has global minima at $(x_1^*, x_2^*) = (-0.0898, 0.7127)$ and $(x_1^*, x_2^*) = (0.0898, -0.7127)$, respectively, where it attains the value $f^* = -1.0316$, and other local optima are not present.

The results of the applied algorithms are summarized in Tables 2(a) and 2(b). Initially four sample sites were used in the experimental designs. The tables show that the minimal relative error is reached when using algorithm version 1, and either Inagaki's or Yager's rule. The tables also show that algorithm version 3 results in the lowest maximal relative error.

The box plots in Figures 2(a) and 2(b) illustrate the dispersion of the relative errors of each algorithm version and conflict redistribution rule. The plots show that algorithm version 2 results in the highest dispersions and medians. In general, algorithm version 3, i.e. choosing in every iteration only the best single model as new response surface, reaches the lowest medians most frequently. Noticeable in Figure 2(b) are the higher amount and higher values of outliers compared to Figure 2(a).

Table 2: Camelback function relative errors

(a) Strategy A

| Rule | min | max | mean |
|---|---|---|---|
| D1 | 0.0000 | 0.0298 | 0.0087 |
| Y1 | 0.0000 | 0.0506 | 0.0118 |
| I1 | 0.0000 | 0.0234 | 0.0059 |
| P1 | 0.0000 | 0.0239 | 0.0072 |
| D2 | 0.0000 | 0.1670 | 0.0317 |
| Y2 | 0.0013 | 0.1762 | 0.0510 |
| I2 | 0.0001 | 0.1437 | 0.0372 |
| P2 | 0.0000 | 0.0203 | 0.0069 |
| D3 | 0.0003 | 0.0161 | 0.0053 |
| Y3 | 0.0000 | 0.0133 | 0.0040 |
| I3 | 0.0000 | 0.0187 | 0.0062 |
| P3 | 0.0001 | 0.0136 | 0.0037 |

(b) Strategy B

| Rule | min | max | mean |
|---|---|---|---|
| D1 | 0.0000 | 0.0238 | 0.0079 |
| Y1 | 0.0000 | 0.0164 | 0.0053 |
| I1 | 0.0000 | 0.0276 | 0.0097 |
| P1 | 0.0010 | 0.0411 | 0.0093 |
| D2 | 0.0006 | 0.2684 | 0.0298 |
| Y2 | 0.0008 | 0.0937 | 0.0222 |
| I2 | 0.0006 | 0.2641 | 0.0359 |
| P2 | 0.0001 | 0.0233 | 0.0055 |
| D3 | 0.0000 | 0.0152 | 0.0040 |
| Y3 | 0.0000 | 0.0189 | 0.0038 |
| I3 | 0.0002 | 0.0274 | 0.0051 |
| P3 | 0.0001 | 0.0182 | 0.0050 |

The weights of the models contributing to the combined response surface in algorithm version 1 were highest for Kriging and RBF. The influence of the MARS model was lowest. Similar to the case of the Branin function the Kriging model is used in most cases after the algorithm switched to using only the best single model. The RBF model was chosen in a few more cases compared to the Branin function. The weights assigned to the single models in algorithm version 2 reflect that the Kriging model had in general the highest influence. RBF and the polynomial model had about the same impact, and the MARS model had again the lowest weights when contributing to the mixture models. In algorithm version 3 the Kriging model was chosen in most cases. The polynomial and MARS model had in comparison to other models the worst characteristics and were thus rarely chosen.

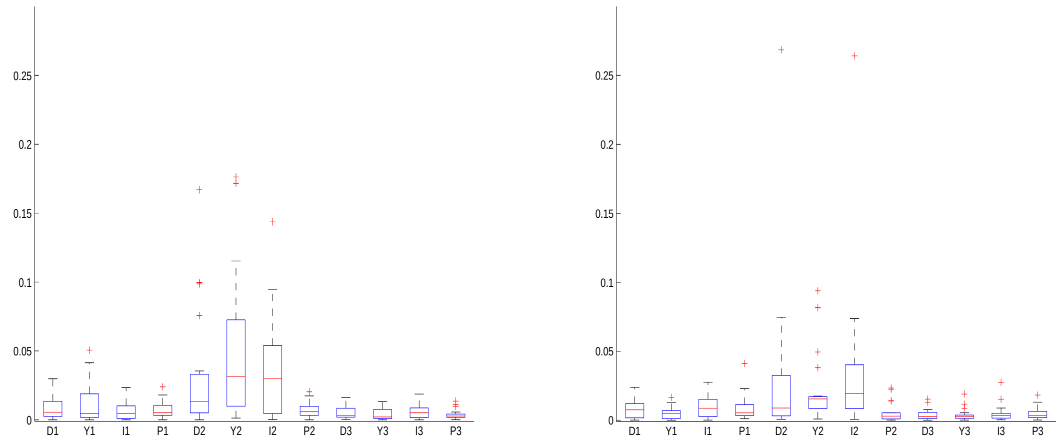

(a) Strategy A

(b) Strategy B

Fig. 2: Camelback function: distribution of relative errors

## 4.3 Test Problem G: Goldstein-Price Function

The variable bounds in this problem were $x_1, x_2 \in [-2, 2]$ and the function is defined by

$$f(x_1, x_2) = \Big[1 + (x_1 + x_2 + 1)^2 (19 - 14x_1 + 3x_1^2 - 14x_2 + 6x_1x_2 + 3x_2^2)\Big] \times \\ \Big[30 + (2x_1 - 3x_2)^2 (18 - 31x_1 + 12x_1^2 + 48x_2 - 36x_1x_2 + 27x_2^2)\Big] .$$

The function has its global minimum at $(x_1^*, x_2^*) = (0, -1)$ and attains there the value $f^* = 3$. In addition, the function has several local minima. Since the range of the function values is very large, the logarithm of the function values has been used during the calculations. The experimental design contained initially four sample sites.

The data in Tables 3(a) and 3(b) show that the overall lowest minimal relative error of 0.02% was achieved by each algorithm version. With respect to the minimal maximum and mean relative error algorithm versions 2 and 3 proved most successful. The box plots in Figures 3(a) and 3(b) are rather similar for every decision rule, but Figure 3(b) contains more outliers. The dispersion of the errors in both figures is about equal. The results suggest that in general algorithm version 3 should be favored.

The weights assigned to the models contributing to the combination differ from those obtained for the Branin and the Camelback function. The highest weights in the mixture model of algorithm version 1 were assigned to the RBF model. The Kriging model had the second highest influence while the MARS and polynomial model were rather insignificant in most cases. After the switch to using only the best single model RBF was chosen in over 90% of all cases. Also in algorithm version 2 the RBF model had significantly higher weights than the other models, and the weights of the Kriging and the polynomial model were in many cases about equal. Again, the MARS model did not contribute much to the response surface. In algorithm version 3 the RBF model had the best model characteristics in many cases and was thus most often chosen as best single model. Polynomial and MARS model had the worst model characteristics.

Table 3: Goldstein-Price function relative errors

(a) Strategy A

| Rule | min | max | mean |
|---|---|---|---|
| D1 | 0.0014 | 0.1140 | 0.0345 |
| Y1 | 0.0058 | 0.1128 | 0.0394 |
| I1 | 0.0012 | 0.0789 | 0.0263 |
| P1 | 0.0002 | 0.1061 | 0.0277 |
| D2 | 0.0002 | 0.1421 | 0.0415 |
| Y2 | 0.0002 | 0.0739 | 0.0212 |
| I2 | 0.0006 | 0.1363 | 0.0372 |
| P2 | 0.0003 | 0.1370 | 0.0301 |
| D3 | 0.0002 | 0.0956 | 0.0214 |
| Y3 | 0.0002 | 0.0822 | 0.0303 |
| I3 | 0.0002 | 0.0887 | 0.0182 |
| P3 | 0.0024 | 0.1130 | 0.0312 |

(b) Strategy B

| Rule | min | max | mean |
|---|---|---|---|
| D1 | 0.0002 | 0.2545 | 0.0393 |
| Y1 | 0.0011 | 0.1185 | 0.0327 |
| I1 | 0.0001 | 0.2367 | 0.0413 |
| P1 | 0.0002 | 0.1185 | 0.0349 |
| D2 | 0.0013 | 0.0615 | 0.0219 |
| Y2 | 0.0002 | 0.1268 | 0.0416 |
| I2 | 0.0002 | 0.2196 | 0.0492 |
| P2 | 0.0039 | 0.3605 | 0.0555 |
| D3 | 0.0013 | 0.0615 | 0.0219 |
| Y3 | 0.0001 | 0.0738 | 0.0220 |
| I3 | 0.0002 | 0.0962 | 0.0161 |
| P3 | 0.0002 | 0.0806 | 0.0181 |

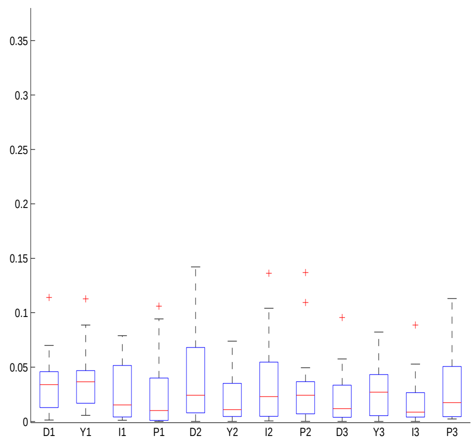

(a) Strategy A

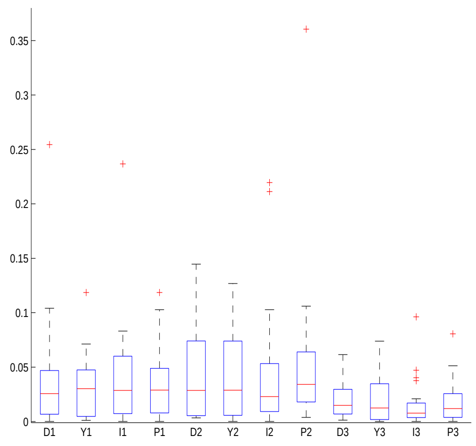

(b) Strategy B

Fig. 3: Goldstein-Price function: distribution of relative errors

### 4.4 Test Problem H3: Three-Dimensional Hartman Function

The class of Hartman functions is defined by

$$f(\mathbf{x}) = -\sum_{i=1}^{m} c_i \exp\left\{-\sum_{j=1}^{k} a_{ij}(x_j - p_{ij})^2\right\},$$

where $\mathbf{x} = (x_1, x_2, \ldots, x_k)$ and $x_i \in [0,1], \forall i$. $m$ has been set to four. The parameters for the three-dimensional problem are given in Table 4.

Table 4: Parameter settings for three-dimensional Hartman function

| $i$ | $a_{ij}$ | | | $c_i$ | $p_{ij}$ | | |
|---|---|---|---|---|---|---|---|
| 1 | 3.0 | 10 | 30 | 1.0 | 0.3689 | 0.1170 | 0.2673 |
| 2 | 0.1 | 10 | 35 | 1.2 | 0.4699 | 0.4387 | 0.7470 |
| 3 | 3.0 | 10 | 30 | 3.0 | 0.1091 | 0.8732 | 0.5547 |
| 4 | 0.1 | 10 | 35 | 3.2 | 0.0382 | 0.5743 | 0.8828 |

This function attains its global optimum $f^* = -3.8628$ at the point $(x_1^*, x_2^*, x_3^*) = (0.1146, 0.5556, 0.8525)$. The function has four local minima. The results of the three versions of the algorithm are presented in Tables 5(a) and 5(b). Five points were used as initial experimental design. The data shows that the overall minimal relative error was achieved when using algorithm version 2. Algorithm versions 2 and 3 give in general better results than version 1. Noticeable is that the results in Table 5(b) are especially for version 1 and 3 better than the corresponding values in Table 5(a).

The differences between the distributions of the relative errors illustrated in Figures 4(a) and 4(b) are rather negligible with respect to dispersion and median values. In general Yager's rule for algorithm version 2 seems to lead to the best results with respect to median and dispersion of the errors.

Table 5: Three-dimensional Hartman function relative errors

(a) Strategy A

| Rule | min | max | mean |
|---|---|---|---|
| D1 | 0.0002 | 0.0134 | 0.0040 |
| Y1 | 0.0006 | 0.0171 | 0.0047 |
| I1 | 0.0009 | 0.0109 | 0.0040 |
| P1 | 0.0001 | 0.0093 | 0.0039 |
| D2 | 0.0001 | 0.0070 | 0.0028 |
| Y2 | 0.0001 | 0.0091 | 0.0032 |
| I2 | 0.0002 | 0.0058 | 0.0026 |
| P2 | 0.0001 | 0.0068 | 0.0025 |
| D3 | 0.0001 | 0.0061 | 0.0028 |
| Y3 | 0.0001 | 0.0054 | 0.0028 |
| I3 | 0.0001 | 0.0116 | 0.0033 |
| P3 | 0.0001 | 0.0113 | 0.0032 |

(b) Strategy B

| Rule | min | max | mean |
|---|---|---|---|
| D1 | 0.0002 | 0.0093 | 0.0034 |
| Y1 | 0.0005 | 0.0121 | 0.0043 |
| I1 | 0.0001 | 0.0106 | 0.0030 |
| P1 | 0.0005 | 0.0083 | 0.0034 |
| D2 | 0.0001 | 0.0065 | 0.0021 |
| Y2 | 0.0009 | 0.0129 | 0.0035 |
| I2 | 0.0001 | 0.0096 | 0.0025 |
| P2 | 0.0004 | 0.0069 | 0.0031 |
| D3 | 0.0005 | 0.0062 | 0.0024 |
| Y3 | 0.0001 | 0.0054 | 0.0023 |
| I3 | 0.0006 | 0.0059 | 0.0028 |
| P3 | 0.0001 | 0.0069 | 0.0027 |

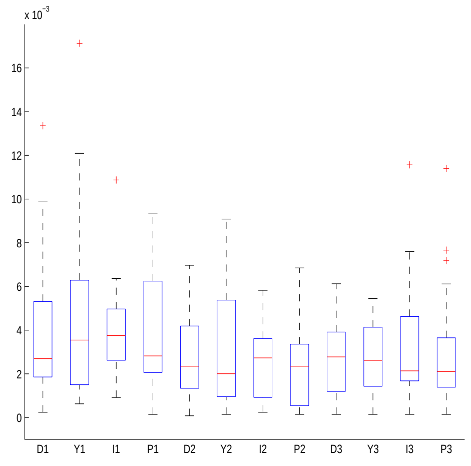

(a) Strategy A

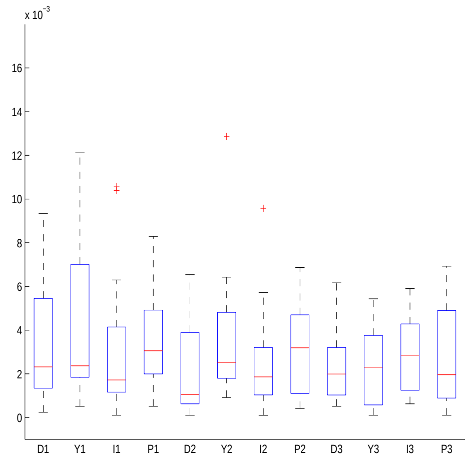

(b) Strategy B

Fig. 4: Three-dimensional Hartman function: distribution of relative errors

For the three-dimensional Hartman function the Kriging model obtained the highest weights when using mixture models in algorithm versions 1 and 2. For algorithm version 1 the weights for the MARS model were higher than for any other already considered test function. The weights of the polynomial model were lowest.

On the other hand, in algorithm version 2 the weight of the MARS model was again comparatively low, and the influence of the Kriging model had increased compared to version 1. When only the best single model was used, the Kriging model was chosen in over 90% of all cases.

## 4.5 Test Problem H6: Six-Dimensional Hartman Function

The parameters of the six-dimensional problem are given in Table 6.

Table 6: Parameters for six-dimensional Hartman function

| $i$ | $a_{ij}$ | | | | | | $c_i$ | $p_{ij}$ | | | | | |
|---|---|---|---|---|---|---|---|---|---|---|---|---|---|
| 1 | 10.0 | 3.0 | 17.0 | 3.5 | 1.7 | 8.0 | 1.0 | 0.1312 | 0.1696 | 0.5569 | 0.0124 | 0.8283 | 0.5886 |
| 2 | 0.05 | 10.0 | 17.0 | 0.1 | 8.0 | 14.0 | 1.2 | 0.2329 | 0.4135 | 0.8307 | 0.3736 | 0.1004 | 0.9991 |
| 3 | 3.0 | 3.5 | 1.7 | 10.0 | 17.0 | 8.0 | 3.0 | 0.2348 | 0.1451 | 0.3522 | 0.2883 | 0.3047 | 0.665 |
| 4 | 17.0 | 8.0 | 0.05 | 10.0 | 0.1 | 14.0 | 3.2 | 0.4047 | 0.8828 | 0.8732 | 0.5743 | 0.1091 | 0.0381 |

The function reaches its global minimum $f^* = -3.3224$ at $(x_1^*, x_2^*, x_3^*, x_4^*, x_5^*, x_6^*) = (0.2017, 0.1500, 0.4769, 0.2753, 0.3117, 0.6573)$, and it has six local optima. The three versions of the algorithm applied to the six-dimensional Hartman function delivered the results shown in Tables 7(a) and 7(b), respectively. Initially eight points were used in the experimental design. The results show that algorithm version 1 achieves the lowest minimal relative errors for most conflict redistribution rules. The tables also show that algorithm versions 1 and 2 give worse results when Holmström's criterion, i.e. strategy A, is used for adding the minimum site of the response surface. Noticeable is that the solution quality has in general decreased compared to the previously considered test problems. Box plots of the relative errors are illustrated in Figures 5(a) and 5(b). The results let conclude that it seems reasonable to use algorithm version 1.

Table 7: Six-dimensional Hartman function relative errors

(a) Strategy A

| Rule | min | max | mean |
|---|---|---|---|
| D1 | 0.0015 | 0.1032 | 0.0388 |
| Y1 | 0.0013 | 0.1007 | 0.0311 |
| I1 | 0.0029 | 0.1130 | 0.0415 |
| P1 | 0.0045 | 0.0963 | 0.0477 |
| D2 | 0.0030 | 0.1073 | 0.0538 |
| Y2 | 0.0043 | 0.1251 | 0.0470 |
| I2 | 0.0040 | 0.1374 | 0.0501 |
| P2 | 0.0058 | 0.1289 | 0.0689 |
| D3 | 0.0027 | 0.0827 | 0.0383 |
| Y3 | 0.0017 | 0.0844 | 0.0403 |
| I3 | 0.0049 | 0.0966 | 0.0477 |
| P3 | 0.0012 | 0.0895 | 0.0563 |

(b) Strategy B

| Rule | min | max | mean |
|---|---|---|---|
| D1 | 0.0020 | 0.0889 | 0.0419 |
| Y1 | 0.0021 | 0.1138 | 0.0325 |
| I1 | 0.0016 | 0.0952 | 0.0408 |
| P1 | 0.0018 | 0.0955 | 0.0380 |
| D2 | 0.0015 | 0.1281 | 0.0639 |
| Y2 | 0.0039 | 0.1130 | 0.0610 |
| I2 | 0.0017 | 0.1300 | 0.0438 |
| P2 | 0.0035 | 0.1544 | 0.0533 |
| D3 | 0.0022 | 0.0978 | 0.0375 |
| Y3 | 0.0061 | 0.0942 | 0.0465 |
| I3 | 0.0028 | 0.0960 | 0.0432 |
| P3 | 0.0035 | 0.1129 | 0.0538 |

The weights determined for the models contributing to combinations in algorithm version 1 show that the Kriging model has the highest contribution (50-60%). For this test problem also the MARS model had influence on the response surface in several cases and did not obtain the lowest weights. In the second phase of algorithm version 1 the Kriging model was chosen by every decision rule in every iteration. In algorithm version 2 again the Kriging model had the highest influence, while MARS and polynomial model had the lowest weights. In algorithm version 3 the Kriging model was chosen in almost 90% of all iterations, and the polynomial and MARS model were rarely used.

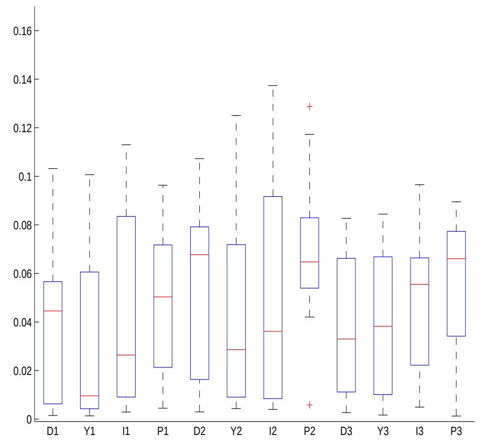

(a) Strategy A

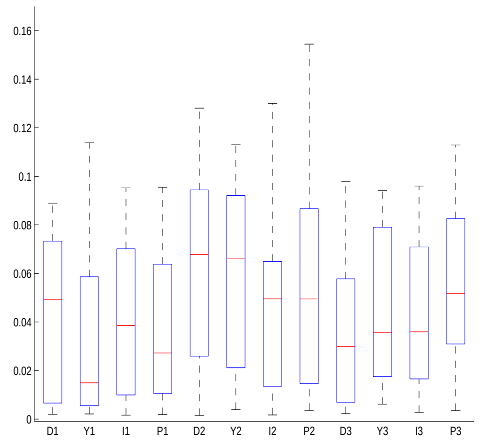

(b) Strategy B

Fig. 5: Six-dimensional Hartman function: distribution of relative errors

## 4.6 Test Problem S: Shekel Function

The general definition of this function type is

$$f(\mathbf{x}) = \sum_{i=1}^{m} \frac{1}{c_i + \sum_{j=1}^{k}(x_j - a_{ji})^2},$$

and the variables are bounded to $\mathbf{x} \in [0, 10]$. The parameters are

$$\mathbf{A} = \begin{bmatrix} 4 & 1 & 8 & 6 & 3 & 2 & 5 & 8 & 6 & 7 \\ 4 & 1 & 8 & 6 & 7 & 9 & 5 & 1 & 2 & 3.6 \\ 4 & 1 & 8 & 6 & 3 & 2 & 3 & 8 & 6 & 7 \\ 4 & 1 & 8 & 6 & 7 & 9 & 3 & 1 & 2 & 3.6 \end{bmatrix}, \text{ and } \mathbf{c} = \frac{1}{10}\,[1, 2, 2, 4, 4, 6, 3, 7, 5, 5]'\,.$$

The Shekel functions have a very steep global minimum at $x_i = 4, \forall i$. In the four-dimensional case the optimal function value is $f^* = -10.5364$, and the number of local optima is $m$, which is in the considered case 10.

The initial experimental design contained 16 points. All versions of the algorithm had trouble finding the global optimum (see Tables 8(a) and 8(b)). The overall best results were achieved by algorithm version 1 in both tables. The results in Table 8(b) are in several cases better than the corresponding entries in Table 8(a).

Figures 6(a) and 6(b) show the distribution of the relative errors for each algorithm version and conflict redistribution rule. Compared to all other previously considered test problems, the results are much worse. The box plots in Figure 6(b) have more outliers than those in Figure 6(a), but otherwise there are no significant differences between strategies A and B.

Also for this test function the weights assigned to the Kriging model were highest in algorithm version 1. The MARS model obtained the lowest weights. However, the difference between the weights for Kriging, polynomial and RBF model was much smaller than for the previously considered test problems. After the switch to using only the best single model Kriging was chosen in most cases, but also RBF had in several cases the best model characteristics. The polynomial and MARS model have never obtained a better evaluation than Kriging or RBF. The same statements hold for algorithm versions 2 and 3. The weights of the models in version 2 were on average as for the first stage of algorithm version 1. In version 3 Kriging and RBF were chosen as best models most often.

Table 8: Shekel function relative errors

(a) Strategy A

| Rule | min | max | mean |
|---|---|---|---|
| D1 | 0.2693 | 0.8130 | 0.6526 |
| Y1 | 0.3360 | 0.8209 | 0.5927 |
| I1 | 0.2973 | 0.8362 | 0.6705 |
| P1 | 0.1483 | 0.8357 | 0.6049 |
| D2 | 0.3966 | 0.8427 | 0.6412 |
| Y2 | 0.4565 | 0.8020 | 0.7035 |
| I2 | 0.3966 | 0.8129 | 0.6418 |
| P2 | 0.4565 | 0.8326 | 0.6847 |
| D3 | 0.3020 | 0.8069 | 0.6360 |
| Y3 | 0.2352 | 0.8372 | 0.6296 |
| I3 | 0.2663 | 0.8296 | 0.6736 |
| P3 | 0.3462 | 0.8126 | 0.6216 |

(b) Strategy B

| Rule | min | max | mean |
|---|---|---|---|
| D1 | 0.1051 | 0.8267 | 0.6657 |
| Y1 | 0.2055 | 0.8179 | 0.6305 |
| I1 | 0.2023 | 0.7987 | 0.5808 |
| P1 | 0.2955 | 0.8581 | 0.6390 |
| D2 | 0.3726 | 0.7888 | 0.6287 |
| Y2 | 0.4565 | 0.8270 | 0.7106 |
| I2 | 0.3699 | 0.8373 | 0.6464 |
| P2 | 0.3726 | 0.8278 | 0.6225 |
| D3 | 0.1300 | 0.7971 | 0.6124 |
| Y3 | 0.2857 | 0.7888 | 0.6371 |
| I3 | 0.2611 | 0.8265 | 0.6189 |
| P3 | 0.3102 | 0.8396 | 0.6014 |

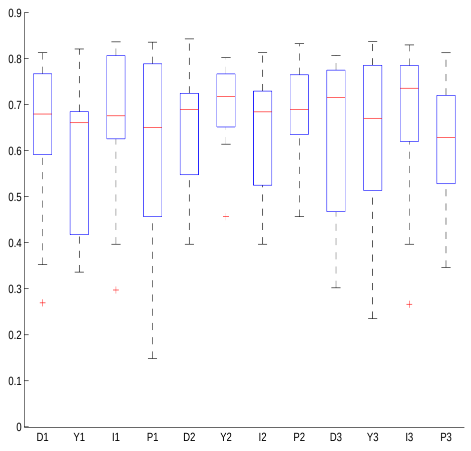

(a) Strategy A

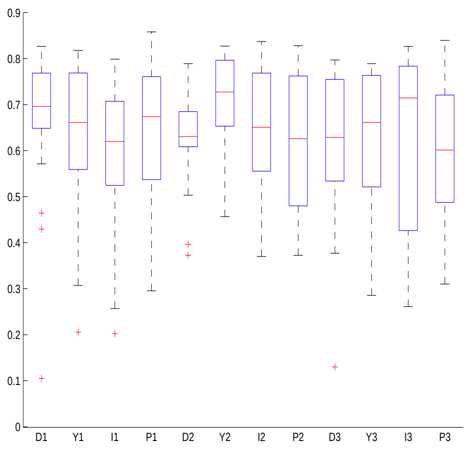

(b) Strategy B

Fig. 6: Shekel function: distribution of relative errors

## 4.7 General Results

The computation time is for all test problems highest whenever only the mixture model was used and lowest when using the best single model. The reason is that the mixture models require the predictions of more than one model, and thus the computation time is higher than when the predictions of only one model are used. With respect to conflict redistribution rules there was in general no difference in computation times.

As mentioned on page 5, the set representing complete ignorance, which is in the considered context the combination of all four models, had to be considered separately since it always has belief and plausibility values equal to one. Thus, algorithm versions 1 and 2 were adjusted so that in every iteration the 4-model mixture was used. Comparing the obtained results for all test problems to the reported results in the foregoing sections showed that there were only a few instances in which the 4-model mixture achieved better results. In general the 4-model mixture resulted in significantly higher maximal relative errors and also the dispersion of the relative errors was larger. The influence of the single models in the combination was highest for Kriging and/or RBF, respectively. Compared to the other algorithm versions the weights for MARS and polynomial model were in general higher than in the previously described results and both models had always about the same influence. Thus, it can be concluded that using in every iteration the 4-model mixture does not lead to improved results.

In addition to investigating how close the algorithms get to the global optima with respect to relative errors, it is of interest if and how many global optima could be detected. Tables 9(a) and 9(b) show the fractions each algorithm was able to sample in the vicinity of the global minima. The vicinity was here defined in terms of the distance of the sample sites to the known locations of global and local optima. The tables show that for the Goldstein-Price and the three-dimensional Hartman function, all algorithm versions found the vicinity of the corresponding global minima without getting trapped in local optima. As the results show, algorithm version 3 found the highest number of global minima for all decision rules when the problem dimension is at most three. However, for higher dimensions algorithm versions 2 and 1 are more successful.

In general the PCR5 rule proved the most successful with respect to the number of global minima found. Compared to the quality of the results however, the PCR5 rule was not always the best, i.e. PCR5 did not always lead to the lowest errors. Interesting are the results for the Shekel function. The lowest relative error obtained was 10.51% by Dempster's conflict redistribution rule and using algorithm version 1. However, all algorithms found the vicinity of the global minima in 50-95% of all test cases, but still the relative errors are not very satisfying. Thus, it can be concluded that the algorithms failed in searching thoroughly locally, and thus they missed the very steep optimum of this function. Therefore, the local search strategy of the algorithms must be enhanced so that also the relative errors for such functions can be decreased.

Comparing the entries of Tables 9(a) and 9(b) shows that the number of global minima found was higher when using Holmström's criterion for adding the minimum site of the response surface. Based on these and the foregoing results (i.e. tables and figures corresponding to strategy A) it seems reasonable to employ Holmström's criterion. On the other hand, since the algorithm versions 1 and 2 proved more successful with increasing dimensions, they should also be used for problems containing more than six variables.

Table 9: Number of basins of global optima found (in %)

(a) Strategy A

| Rule | B | C | G | H3 | S | H6 |
|---|---|---|---|---|---|---|
| D1 | 91.67 | 95.00 | 100.00 | 100.00 | 65.00 | 85.00 |
| Y1 | 76.67 | 100.00 | 100.00 | 100.00 | 75.00 | 95.00 |
| I1 | 86.67 | 100.00 | 100.00 | 100.00 | 50.00 | 80.00 |
| P1 | 83.33 | 100.00 | 100.00 | 100.00 | 70.00 | 80.00 |
| D2 | 86.67 | 65.00 | 100.00 | 100.00 | 85.00 | 80.00 |
| Y2 | 83.33 | 57.50 | 100.00 | 100.00 | 60.00 | 90.00 |
| I2 | 81.67 | 72.50 | 100.00 | 100.00 | 75.00 | 90.00 |
| P2 | 81.67 | 100.00 | 100.00 | 100.00 | 75.00 | 85.00 |
| D3 | 96.67 | 100.00 | 100.00 | 100.00 | 60.00 | 80.00 |
| Y3 | 96.67 | 100.00 | 100.00 | 100.00 | 60.00 | 80.00 |
| I3 | 95.00 | 100.00 | 100.00 | 100.00 | 50.00 | 85.00 |
| P3 | 100.00 | 100.00 | 100.00 | 100.00 | 65.00 | 70.00 |

(b) Strategy B

| Rule | B | C | G | H3 | S | H6 |
|---|---|---|---|---|---|---|
| D1 | 85.00 | 100.00 | 100.00 | 100.00 | 55.00 | 75.00 |
| Y1 | 81.67 | 97.50 | 100.00 | 100.00 | 65.00 | 85.00 |
| I1 | 85.00 | 95.00 | 100.00 | 100.00 | 75.00 | 85.00 |
| P1 | 83.33 | 100.00 | 100.00 | 100.00 | 65.00 | 80.00 |
| D2 | 81.67 | 77.50 | 100.00 | 100.00 | 80.00 | 90.00 |
| Y2 | 81.67 | 80.00 | 100.00 | 100.00 | 45.00 | 85.00 |
| I2 | 25.00 | 82.50 | 100.00 | 100.00 | 70.00 | 85.00 |
| P2 | 81.67 | 100.00 | 100.00 | 100.00 | 60.00 | 85.00 |
| D3 | 96.67 | 100.00 | 100.00 | 100.00 | 60.00 | 80.00 |
| Y3 | 96.67 | 100.00 | 100.00 | 100.00 | 50.00 | 85.00 |
| I3 | 95.00 | 100.00 | 100.00 | 100.00 | 45.00 | 80.00 |
| P3 | 100.00 | 100.00 | 100.00 | 100.00 | 65.00 | 65.00 |

Tables 10(a) and 10(b) show the minimum number of true function evaluations that were necessary to reach relative errors of less than 1% in all 20 runs (note that the Shekel test function is not included since relative errors of less than 1% were not achieved). The numbers show that Inagaki's as well as the PCR5 rule are most successful when using algorithm version 1. For algorithm version 2 Yager's rule proved most often successful, and Dempster's rule worked best when algorithm version 3 was used. Comparing the overall performance of all conflict redistribution rules shows that Inagaki's rule is the most promising.

Tables 11(a) and 11(b) show the number of simulations in which relative errors of less than 1% have been reached, i.e. in how many of the 20 simulation runs of each method for every problem the global optimum could be approximated with an error of less than 1%. For example, with Strategy A the method D1 found for the test problem B in 10 out of 20 simulation runs the global optimum with an error of less than 1%. For algorithm version 1 again Inagaki's rule is most successful, while Dempster's or Yager's rule are recommendable when

Table 10: Minimum number of function evaluations to reach less than 1% relative error

(a) Strategy A

| Rule | B | C | G | H3 | H6 |
|---|---|---|---|---|---|
| D1 | 26 | 15 | 47 | 30 | 72 |
| Y1 | 23 | 22 | 52 | 19 | 56 |
| I1 | 12 | 22 | 39 | 20 | 40 |
| P1 | 27 | 10 | 33 | 16 | 67 |
| D2 | 23 | 16 | 46 | 21 | 70 |
| Y2 | 12 | 15 | 42 | 14 | 60 |
| I2 | 25 | 14 | 50 | 18 | 63 |
| P2 | 27 | 9 | 65 | 21 | 58 |
| D3 | 12 | 17 | 29 | 17 | 62 |
| Y3 | 27 | 25 | 46 | 22 | 96 |
| I3 | 21 | 9 | 29 | 21 | 129 |
| P3 | 14 | 21 | 42 | 20 | 102 |

(b) Strategy B

| Rule | B | C | G | H3 | H6 |
|---|---|---|---|---|---|
| D1 | 33 | 24 | 22 | 22 | 79 |
| Y1 | 17 | 10 | 54 | 18 | 101 |
| I1 | 14 | 22 | 19 | 13 | 37 |
| P1 | 25 | 24 | 29 | 17 | 66 |
| D2 | 17 | 24 | 49 | 24 | 79 |
| Y2 | 12 | 15 | 40 | 19 | 51 |
| I2 | 27 | 8 | 69 | 20 | 71 |
| P2 | 17 | 11 | 48 | 20 | 88 |
| D3 | 12 | 15 | 30 | 19 | 51 |
| Y3 | 25 | 16 | 29 | 28 | 62 |
| I3 | 13 | 22 | 36 | 20 | 89 |
| P3 | 15 | 23 | 22 | 22 | 64 |

using algorithm version 2. For algorithm version 3 Dempster's rule works best. An overall comparison of the results of all conflict redistribution rules shows that Yager's and the PCR5 rule have the best performance. Thus, together with the results from Tables 10 it seems promising to use Inagaki's rule when algorithm version 1 is used, Yager's rule in algorithm version 2, and Dempster's rule with algorithm version 3 in order to obtain the best results.

Table 11: Number of simulations in which less than 1% relative error found

(a) Strategy A

| Rule | B | C | G | H3 | H6 |
|---|---|---|---|---|---|
| D1 | 10 | 14 | 4 | 19 | 7 |
| Y1 | 17 | 8 | 5 | 20 | 3 |
| I1 | 13 | 15 | 10 | 20 | 5 |
| P1 | 6 | 13 | 3 | 18 | 10 |
| D2 | 16 | 5 | 10 | 20 | 6 |
| Y2 | 16 | 18 | 6 | 20 | 5 |
| I2 | 9 | 15 | 9 | 19 | 6 |
| P2 | 19 | 7 | 8 | 20 | 5 |
| D3 | 13 | 16 | 11 | 19 | 3 |
| Y3 | 9 | 13 | 10 | 20 | 2 |
| I3 | 13 | 15 | 7 | 20 | 1 |
| P3 | 13 | 18 | 7 | 19 | 2 |

(b) Strategy B

| Rule | B | C | G | H3 | H6 |
|---|---|---|---|---|---|
| D1 | 7 | 11 | 8 | 20 | 7 |
| Y1 | 14 | 10 | 7 | 20 | 2 |
| I1 | 15 | 18 | 6 | 20 | 6 |
| P1 | 9 | 16 | 6 | 18 | 9 |
| D2 | 16 | 7 | 7 | 19 | 2 |
| Y2 | 11 | 16 | 7 | 20 | 2 |
| I2 | 7 | 12 | 4 | 18 | 5 |
| P2 | 12 | 7 | 6 | 20 | 4 |
| D3 | 14 | 18 | 13 | 20 | 2 |
| Y3 | 11 | 13 | 6 | 20 | 5 |
| I3 | 17 | 16 | 4 | 20 | 2 |
| P3 | 13 | 16 | 10 | 20 | 4 |

## 5 Conclusions and Future Research Topics

This paper has presented the application of Dempster-Shafer theory to surrogate model choice and surrogate model combination in global optimization problems. Model characteristics obtained from cross validation reflect good and bad properties of the considered models and their combinations, respectively. Different rules for redistributing the conflict originating from good and bad properties of the same model have been considered and compared. The advantage of this approach is that no parameters need to be adjusted in order to emphasize or restrict the influence of conflicting model characteristics. Also the impact of the usage of mixture models, single models and a combination of both have been examined and results compared on global optimization test problems.

The results showed that the proposed approach proved successful in finding the global minima of most test problems. The exploration of the variable domain had a good ratio of local and global search, and thus the vicinities of global minima were detected and the actual global minimum could, with the exception of one test function, be found with average relative errors of less than 1%. The algorithms had trouble only with the test function which had a very steep global minimum. Although the vicinity of the global minimum has been detected and several samples have been taken in the prospective region, the algorithm failed to search thoroughly enough in order to find the actual location of the minimum. This implies that the used local search procedure should still be improved in order to detect also very steep minima. In connection with this issue is also the adjustment of parameters determining for example when to invoke the local search, how many new sample sites should be taken, or the definition of the search area when optimizing the auxiliary function.

The results also indicated that the success of the algorithms in finding all global minima was to some extent dependent on the used conflict redistribution rule and the algorithm version. In general, the proportional conflict redistribution rule led to the best variable domain exploration. On the other hand, this rule did not always lead to the lowest relative errors, and thus the possibility of linking the conflict redistribution rule to the search phase (local or global) should be examined in further experiments. With respect to variable domain exploration and relative errors the results showed that with increasing problem dimension the algorithms applying model combinations become more favorable. However, this issue should further be examined in real-world application problems. The amount and type of model characteristics used for the evaluation of the goodness of the single surrogate models should then also be derived from the specific application, i.e. in some cases certain model characteristics may be more important than others and should thus be emphasized in the model evaluation. In connection with real-world applications is also the extension of the algorithms to handling linear and nonlinear constraints as well as integer conditions which can be assumed to be present in most engineering problems. Further testing of the implemented procedures on higher dimensional problems and an analysis of their efficiency is necessary. The testing showed that there are in general no major differences in computation times when using different conflict redistribution rules. Differences arise only when using single or mixture models as response surfaces. In general it can be assumed that evaluating the true function is much more costly than building the surrogate models, and thus the described approach is feasible also with respect to computation times.

With respect to the computational demand the described algorithms are suitable for distributed computing. For example the cross validation of the single models is an "embarrassingly parallel" computation, as is the procedure for minimizing the auxiliary functions and the response surface. In case the cross validation becomes computationally too expensive, it is possible to consider the re-evaluation and choice of the best model only every, say, $l$th iteration, or to switch to a $k$-fold cross validation strategy after a certain number of samples has been obtained. An important issue connected with the first possibility is the determination of $l$, i.e. how often the (mixture) model should be re-adjusted while keeping the solution quality at a high level. These extensions of the algorithms will be considered in future developments.

**Acknowledgements**

We would like to thank the anonymous reviewers for their helpful comments.

## References

1. M. J. Appel, R. Labarre, and D. Radulović. On accelerated random search. *SIAM Journal on Optimization*, 14708-731, 2003.
2. M. Björkman and K. Holmström. Global optimization of costly nonconvex functions using radial basis functions. *Optimization and Engineering*, 1:373–397, 2001.
3. C. Currin, T. Mitchell, M. Morris, and D. Ylvisaker. A bayesian approach to the design and analysis of computer experiments. Technical report, Oak Ridge National Laboratory, Oak Ridge, TN, 1988.
4. A. P. Dempster. A generalization of bayesian inference. *Journal of the Royal Statistical Society*, Series B 30:205–247, 1968.

5. J. Duchon. *Constructive Theory of Functions of Several Variables.* Springer-Verlag, Berlin, 1977.
6. J. H. Friedman. Multivariate adaptive regresion splines. *The Annals of Statistics*, 19:1–141, 1991.
7. B. Glaz, P.P. Friedmann, and L. Liu. Surrogate based optimization of helicopter rotor blades for vibration reduction in forward flight. *Structural and Multidisciplinary Optimization*, 35:341–363, 2008.
8. T. Goel, R. T. Haftka, W. Shyy, and N. V. Queipo. Ensemble of surrogates. *Structural Multidisciplinary Optimization*, 33:199–216, 2007.
9. K. Holmström. An adaptive radial basis algorithm (ARBF) for expensive black-box global optimization. *Journal of Global Optimization*, 41:447–464, 2008.
10. T. Inagaki. Interdependence between safety-control policy and multiple-sensor schemes via Dempster-Shafer theory. *IEEE Transactions on Reliability*, 40:182–188, 1991.
11. D. R. Jones. A taxonomy of global optimization methods based on response surfaces. *Journal of Global Optimization*, 21:345–383, 2001.
12. D. R. Jones, M. Schonlau, and W. J. Welch. Efficient global optimization of expensive black-box functions. *Journal of Global Optimization*, 13:455–492, 1998.
13. X. B. Lam, Y. S. Kim, A. D. Hoang, and C. W. Park. Coupled aerostructural design optimization using the kriging model and integrated multiobjective optimization algorithm. *Journal of Optimization Theory and Applications*, DOI: 10.1007/s10957-009-9520-9, 2009.
14. X. Liao, Q. Li, X. Yang, W. Zhang, and W. Li. Multiobjective optimization for crash safety design of vehicles using stepwise regression model. *Structural and Multidisciplinary Optimization*, 35:561–569, 2008.
15. S. N. Lopheven, H. B. Nielsen, and J. Søndergaard. DACE a matlab kriging toolbox. Technical report, Technical Report IMM-TR-2002-12, 2002.
16. J.B. MacQueen. Some methods for classification and analysis of multivariate observations. *Proceedings of the Fifth Berkeley Symposium on Mathematical Statistics and Probability, University of California Press*, 1:281–297, 1967.
17. J. D. Martin and T. W. Simpson. Use of kriging models to approximate deterministic computer models. *AIAA Journal*, 43:853–863, 2005.
18. G. Matheron. Principles of geostatistics. *Economic Geology*, 58:1246–1266, 1963.
19. R. C. Morgans, A. C. Zander, C. H. Hansen, and D. J. Murphy. EGO shape optimization of horn-loaded loudspeakers. *Optimization and Engineering*, 9:361–374, 2008.
20. R. H. Myers and D. C. Montgomery. *Response Surface Methodology, Process and Product Optimization using Designed Experiments.* Wiley-Interscience Publication, 1995.
21. M. J. D. Powell. *The Theory of Radial Basis Function Approximation in 1990.* Advances in Numerical Analysis, vol. 2: wavelets, subdivision algorithms and radial basis functions. Oxford University Press, Oxford, pp. 105-210, 1992.
22. M. J. D. Powell. *Recent Research at Cambridge on Radial Basis Functions.* New Developments in Approximation Theory, pp. 215-232. Birkhäuser, Basel, 1999.
23. N. V. Queipo, R. T. Haftka, W. Shyy, T. Goel, R. Vaidyanathan, and P. K. Tucker. Surrogate-based analysis and optimization. *Progress in Aerospace Sciences*, 41:1–28, 2005.
24. R. G. Regis and C. A. Shoemaker. Constrained global optimization of expensive black box functions using radial basis functions. *Journal of Global Optimization*, 31:153–171, 2005.
25. R. G. Regis and C. A Shoemaker. Improved strategies for radial basis function methods for global optimization. *Journal of Global Optimization*, 37:113–135, 2007.
26. G. Shafer. *A Mathematical Theory of Evidence.* Princeton University Press, 1976.
27. F. Smarandache and J. Dezert. Information fusion based on new proportional conflict redistribution rules. In *7th International Conference on Information Fusion, pp. 907-914*, 2005.
28. F. A. C. Viana and R. T. Haftka. Using multiple surrogates for minimization of the RMS error in metamodeling. In *Proceedings of the ASME 2008 International Design Engineering Technical Conferences & Computers and Information in Engineering Conference DETC2008-49240*, 2008.
29. R. R. Yager. On the Dempster-Shafer framework and new combination rules. *Information Sciences*, 41:93–137, 1987.
30. R. J. Yang, N. Wang, C. H. Tho, J. P. Bobineau, and B.P. Wang. Metamodeling development for vehicle frontal impact simulation. *Journal of Mechanical Design*, 127:1014–1021, 2005.
31. L. A. Zadeh. Review of book: A mathematical theory of evidence. *The AI Magazine*, 5:81–83, 1984.
32. P. Zhu, Y. Zhang, and G.-L. Chen. Metamodel-based lightweight design of an automotive front-body structure using robust optimization. *Proceedings of the Institution of Mechanical Engineers, Part D: Journal of Automobile Engineering*, DOI: 10.1243/09544070JAUTO1045, 2009.